Response to the comments by the reviewers
Qingcai Chen, Haoyao Sun and Yanlin Zhang.

We appreciate the comments from two reviewers. We have answered the comments of the two reviewers, and addressed the problems raised by the reviewers, such as inaccurate descriptions of the details of this article and logical problems. These improvements have a very positive effect on this article.

Our responses to all the comments from the reviewers and changes made in the paper are listed below.

Reviewer #1:

EPFRs are widely present in atmospheric particulates, but there is a limited understanding of the size-resolved health risks of these radicals. Here, they reported the risks and sources of EPFRs for different particles in summer and winter. They found different types of sources of EPFRs in particles with different sizes. The experimental design was good, and evidence was solid. The results were useful for scientific community, so this paper can be published after the authors address the following comments.

We appreciate the positive evaluation of this work.

Specific comments:

(1) It is somehow surprising for me that biomass burning was a major emission source in summer. What was the major types of BB? Open burning?

We appreciate this comment from the reviewer. The results from factor analysis shown that EPFRs mainly from the combustion sources both in winter and summer. However, the results also showed that the dominant factors were different in winter and summer. Obviously the winter is coal burning and thus the summer should be other combustion sources instead of burning coal. According to the production structure of Linfen area, wheat is the main local agricultural crop, and there is often a problem of burning wheat straw in summer, so we speculate that biomass burning may be an important source of EPFRs. We note that this result is speculative. We have modified this part as follows:

P2L22-24: “In both seasons, combustion sources are the main sources of EPFRs with coal combustion as the major contributor in winter, while other fuel combustions are the major source in summer.”

P11L258-260: “Factor 2 is different from factor 1; factor 2 is more likely the combustion of fossil fuels, while factor 1 should be other combustion sources instead of burning coal, such as biomass combustion.”

(2) Sec. 2.2 and 2.4 more details should be given.

We appreciate this comment from the reviewer. We have added more details about the analysis of EPFRs and PAHs in the sections of 2.2 and 2.4 as follows:

L103-111 (Sec. 2.2): *EPFR analysis*

The EPR spectrometer (MS5000, Freiberg, Germany) is used to detect EPFRs in atmospheric samples. Cut the sample filter into thin strips (5 mm × 28 mm), and put it into the sample tank of the quartz tissue cell (the size of the sample tank is 10 mm × 30 mm)., Then the quartz tissue cell with attached filter sample was placed in a resonant cavity and analyzed by an EPR spectrometer. The detection parameters were magnetic field strength, 335 - 342 mT; detection time, 60 s; modulation amplitude, 0.20 mT; number of detections, 1; and microwave intensity, 8.0 mW. Specific testing protocols have been described previously (Chen et al., 2018c).

L125-140 (Sec. 2.3): *PAH analysis*

PAHs were detected using gas chromatography/mass spectrometry (GC/MS) on a GC7890B/MS5977A (Agilent Technologies, Clara, CA). Quartz-fiber filter samples (8 mm in diameter) were cut from each 25-mm quartz-fiber filter substrates used on the ELPI impactor stages using a stainless-steel round punch over a clean glass dish and loaded into the TD glass tube. Next, the TD glass tube was heated to 310 °C at a rate of 12 °C/min and thermally desorbed at 310 °C for 3 min. The desorbed organic compounds were trapped on the head of a GC-column (DB-5MS: 5% diphenyl-95% dimethyl siloxane copolymer stationary phase, 0.25-mm i.d., 30-m length, and 0.25-mm thickness). Sixteen target PAHs were identified based on retention time and qualified ions of the standards, including 16 EPA parent PAHs (p-PAHs). The method detection limits (MDLs) ranged from 0.2 pg/mm2 (Ace) to 0.6 pg/mm2 (Incdp). Naphthalene-D8, acenaphthene-D10, phenanthrene-D10, chrysene-D12, and perylene D12 were used for the analytical recovery check. All compounds were recovered with a desorption recovery percentage of > 90%. Specific testing protocols have been described previously (Han et al., 2018).

(3) Line 147: not to use active tense (we or I).

We appreciate this comment from the reviewer. We have modified this part in the whole text as follows:

L161-162: “To assess the health risks of EPFRs, this study divided the …”
L170-171: “In addition, the daily inhaled concentration… were converted.”
L208-210: “In another study, the results have shown …”
L317-319: “To evaluate the health risks…, this study evaluated the …”
L397-399: “Through this study, the results have shown....”
L401-403: “It is found that the upper respiratory tract …”

(4) Lines 181-182: evidence should be given to prove it was coal combustion.

We appreciate this comment from the reviewer. We have modified this part as follows:

L192-196: In addition, the concentration of EPFRs in particulates <0.43 μm in winter is very high, but it is very low in summer. According to the results of factor analysis in part 3.2 of this study, this particulate matter is related to combustion, which indicates that coal combustion in winter may provide an important contribution to EPFRs.

(5) Line 194: it is not necessary dust, and biogenic aerosols can contribute to large particles.

We appreciate this comment from the reviewer. As the reviewer said, biogenic aerosols may be an important contribution to coarse particulate matter, but there is no research on EPFRs in bioaerosols. Previous studies have demonstrated that dust is an important source of EPFRs in atmospheric particulates in these western Regions of China (Chen et al., 2018b and 2019b). So, this study highlights the sources of dust. Thus, as suggested by the reviewer we also add a possible source of bioaerosols as follows:

L207-208: For example, coarse particles are often associated with dust sources and biogenic aerosols.

(6) Line 207: more details should be given to explain g-factor.

We appreciate this comment from the reviewer. We have modified this part as follows:

L220-226: The *g*-factor obtained by using EPR to detect the sample is an important parameter to distinguish the type of EPFR. It is the ratio of the electronic magnetic moment to its angular momentum (Shaltout et al., 2015; Arangio et al., 2016). The *g*-factor of carbon-centered persistent free radicals is generally less than 2.003, the *g*-factor of oxygen-centered persistent radicals is generally greater than 2.004, and the g factor of carbon-centered radicals with adjacent oxygen atoms is between 2.003 and 2.004 (Cruz et al., 2012).

(7) I do not suggest using "first" throughout the text.

We appreciate this comment from the reviewer. As the reviewer said, it is not rigorous enough to use "first" in the full text. We have modified the relevant description in this article.

L17 and L139: "first" has been removed.

L330: “EPFRs were first found in…” has been replaced by “EPFRs were found early in…”

(8) Line 380-389: what can be the implication for such seasonality? what is the driven factor ?

We appreciate this comment from the reviewer. This seasonal characteristic is mainly affected by the source characteristics of EPFRs. For example, in winter, EPFRs are mainly found in fine particles. These EPFRs are not only easier to enter the human body, but also due to the smaller g factor and lower oxidation degree, which means that their reactivity is higher and the harm to the human body is greater. We have added more details about the driven factor and the implication of seasonal characteristic of EPFRs as follows:

L381-383: This seasonal characteristic of EPFRs is mainly affected by the PM sources, this result also indicates that the potential toxicity caused by EPFRs may also vary with particle size and season.

Reviewer #2:

This paper reports measurements of environmentally persistent free radicals (EPFRs) in particulate matter sampled in Linfen, China. The measurements took place in 2 seasons and involved size-resolved samples. The work makes a contribution to our understanding of this unique group of health actors, so should be published pending the authors addressing some general and specifics comments.

We appreciate the positive evaluation of this reviewer.

General Comments:
There are sections of the Result and Discussion that are repetitious and could be better organized and made more concise. I will point those out in the specific comments, and I strongly recommend the authors go through the paper with an eye towards making it more clear. The authors use the term "formation mechanism" throughout the paper, but they present nothing that resembles the chemistry that would constitute a formation mechanism. I think the authors need to find a better term that describes what they mean, or show actual chemical mechanisms.

We appreciate this comment from the reviewer. We have deleted the results and simplified the conclusion part of the article.

Section 4:

"This study systematically reported the particle size distribution of EPFRs in atmospheric PM in Linfen, which is one of the most polluted cities in China and is located in a typical coal-burning area. In addition, this study evaluated the comprehensive health risks of EPFRs, and reported possible sources and formation process of atmospheric EPFRs with respect to different particle sizes. The following main conclusions were obtained.

(1) This study found that EPFRs are widely present in atmospheric particles of different particle sizes and exhibit significant particle size distribution characteristics. The results of this study demonstrate that the concentrations and types of EPFRs are dependent on particle size and season. This seasonal characteristic of EPFRs is mainly affected by the PM sources, this result also indicates that the potential toxicity caused by EPFRs may also vary with particle size and season.

(2) This study reported the possible source and formation process of atmospheric EPFRs in different particle sizes. The results show that combustion is the most important source of EPFRs (>70%) in both winter and summer PM samples in Linfen. The graphite oxide-like process has the highest contribution (~70%) and is mainly distributed in particles with a size of > 0.43 μm. These findings deepen our understanding of the pollution characteristics of atmospheric EPFRs and are useful for controlling EPFR generation in heavily polluted areas.

(3) This study assessed the exposure risk of EPFRs in different areas of the respiratory system. The results show that the upper respiratory tract is the area with

the highest EPFR exposure. The trachea and alveoli are also exposed to EPFRs, and the risk of exposure is equivalent to that of 8 cigarettes per person per day. Coarse particles are the main source of EPFRs in the upper respiratory tract, while fine particles are mainly involved in the alveoli.

Through this study, the results have shown that there are significant differences in the concentrations and types of EPFRs in particles of different sizes and these differences are due to the influence of the source and generation process. In the future, assessments of the particle size distribution and the seasonality of EPFRs in atmospheric PM should be considered. Health risks are another focus of this study. It is found that the upper respiratory tract is the key exposure area of EPFRs, and the traffic source is the main source of EPFRs in this area. This finding is significant for a systematic assessment of the health risks of EPFRs. In view of the complexity and diversity of the formation process of EPFRs in actual atmospheric particulates, the relative contributions of EPFRs generated by different process and their associated health risks should be more comprehensively studied in the future."

In addition, the term generation mechanism is used in many places in this article, and we have changed it to the generation process (includes Key words, L351, L345, etc.). In addition, based on the reviewers' specific comments, we have rewritten some logically problematic parts as follows.

Specific comments:

(1) Line 17: I am always skeptical when people claim 'firsts'. In addition this is phrased in the past tense. Why not just say "This study reports. . ."?

We appreciate this comment from the reviewer. As the reviewer said, it is not rigorous enough to use "first" in the full text. We have modified this part as follows:

L17-19: This study reports the exposure risks and source of EPFRs in atmospheric particulate matter (PM) of different particle sizes (<10 μm) in Linfen, a typical coal-burning city in China.

(2) Lines 101-102: How long were the samples refrigerated before analysis?

We appreciate this comment from the reviewer. The samples used in this study have a low temperature storage time of 1 year before testing. Our previous research has shown that the proportion of long-life EPFRs (with a lifetime of 3-5 years) in atmospheric samples exceeds 80% (Chen et al., 2019). In addition, we compared the EPR spectra of the same sample before and after storage for 1 year. The results showed that EPFRs did not change significantly. Therefore, long-term storage will not affect the conclusions of this study.

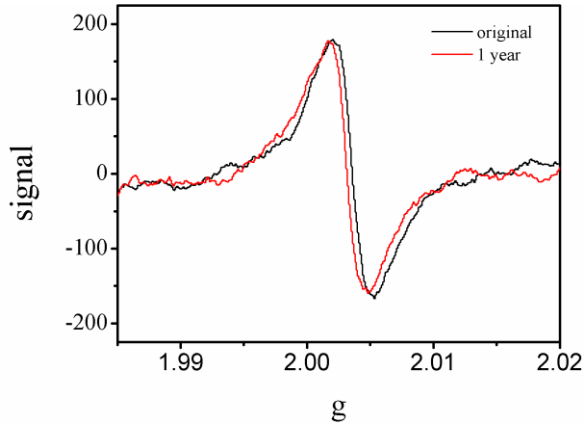

Figure S1 The average EPR spectrum of samples stored before and after 1 year ago. N=9. Sample date: January 25-27, April 20-22, July 11-13 2017. Original refers to the sample used in this article, 1 year means that these samples are stored for 1 year (Chen et al., 2019).

- Chen, Q., Sun, H., Mu, Z., Wang, Y., Li, Y., Zhang, L., Wang, M., Zhang, Z., 2019. Characteristics of environmentally persistent free radicals in PM2.5: Concentrations, species and sources in Xi'an, Northwestern China. Environ. Pollut. 247, 18−26.

(3) Lines 141-142: The phrase "find a solution to the final solution" sounds awkward and should be rephrased.

We appreciate this comment from the reviewer. We have added the discussion of g-factor changes and EPFRs decay as follows:

L153-156: Use the gradient-based multiplication algorithm to find a solution from multiple random starting values, and then use the first algorithm to find the final solution based on the least squares effective set algorithm.

(4) Lines 190-192: The phrasing here is unclear. I think the authors mean the size-segregated contribution of EPFR concentration to the overall. Is this contribution by mass, it's not clear?

We appreciate this comment from the reviewer. This sentence refers to the contribution of EPFRs in coarse and fine particles to the total concentration of EPFRs. We have changed this part as follows:

L204-206: Figure 1b shows the size-segregated contribution of EPFR concentration to the overall. The contribution of fine PM in summer is only 14.9%, while in winter is 58.5%.

(5) Line 195: What kind of EPFRs are found in dust particles? Metals?

We appreciate this comment from the reviewer. Such EPFRs are supposed

mainly as a type of metals. According to our previous research results, EPFRs in sand and dust have no correlation with EC, which may be due to the fact that dust and gravel contain many magnetic materials such as Cu^{2+}, Mn^{2+} and Zn^{2+}. They are not only paramagnetic, but may also react with some organic matter to form EPFRs and attach to atmospheric particles. We have added the kind of EPFRs in the test as follows:

L209: "…particles contain large amounts of metallic EPFRs and that…"

- Chen, Q., Wang, M., Sun, H., Wang, X., Wang, Y., Li, Y., Zhang, L., Mu, Z., 2018b. Enhanced health risks from exposure to environmentally persistent free radicals and the oxidative stress of PM2.5 from asian dust storms in erenhot, Zhangbei and Jinan, China. Environ. Int. 123, 260−268.

(6) Lines 207-233: This paragraph was hard to follow, I think because the authors skipped around from sentence to sentence in their discussion of g-factor, concentration, size fraction and season. Sometimes a sentence would be referring to the previous sentence, but in a way that was hard to follow. I would like to see this section rearranged so that it has a more logical and clear flow. Pick one feature at a time and make sure it is clear in each sentence what is being referred to.

We appreciate this comment from the reviewer. There are some problems with the logic of this paragraph, we have rewritten it as follows:

L220-242: The *g*-factor obtained by using EPR to detect the sample is an important parameter to distinguish the type of EPFR. It is the ratio of the electronic magnetic moment to its angular momentum (Shaltout et al., 2015; Arangio et al., 2016). The *g*-factor of carbon-centered persistent free radicals is generally less than 2.003, the *g*-factor of oxygen-centered persistent radicals is generally greater than 2.004, and the g factor of carbon-centered radicals with adjacent oxygen atoms is between 2.003 and 2.004 (Cruz et al., 2012). Figure 2a shows the *g*-factor distribution characteristics of EPFRs in different particle sizes in summer and winter. The *g*-factor of fine particles and coarse particles shows different characteristics. The *g*-factor of EPFRs in fine particles (particle size < 2.1 μm) ranges from 2.0034 to 2.0037, which may be from carbon-centered radicals with adjacent oxygen atoms. However, the *g*-factor of EPFRs in coarse particles (particle size > 2.1 μm) is significantly less than that of fine particles. The *g*-factor ranges from 2.0031 to 2.0033, indicating that EPFRs in coarse particles are more carbon-centered than those in fine particles and are free of heteroatoms. As shown in Figure 2b, the variation in the *g*-factor with concentration in different season is different. The *g*-factor of summer PM showed a significant decreasing trend with increasing concentration, while the *g*-factor of winter PM showed a significant increasing trend with increasing EPFR concentration. Oyana et al. (2017) studied EPFRs in the surface dust of leaves in the Memphis region of the United States and found that the concentration of EPFRs was positively correlated with the *g*-factor, and they believed that this was related to the source of EPFRs. This

phenomenon indicates that the sources and toxicity of EPFRs in winter and summer are different.

(7) Lines 244: Could it be that the POC in these samples is actually from secondary organic aerosol formation?

We appreciate this comment from the reviewer. The dominant factor of factor 1 is WISOC, which is typical of a primary combustion source. On the one hand, according to the generation characteristics of EPFRs, the dominant component of the aromatic substances EPFRs produced by low-temperature combustion. On the other hand, according to the local pollution characteristics, summer burning mainly comes from the burning of straw and the catering process. Therefore, we believe that factor one may be mainly biomass combustion. According to previous studies, EPFRs generated by the secondary process are usually active, with a life span of only tens of minutes, so it is unlikely that they are secondary aerosols.

- Chen, Q., Sun, H., Wang, M., Wang, Y., Zhang, L., Han, Y., 2019. Environmentally persistent free radical (EPFR) formation by visible-light illumination of the organic matter in atmospheric particles. Environ. Sci. Technol, 53 (17), 10053−10061.

(8) Lines 254-256: Here the authors are talking about a graphite oxide formation mechanism – this would be greatly improved if they could should the actual chemical reactions – that is what constitutes a mechanism.

We appreciate this comment from the reviewer. The research on the chemical reaction of the generation mechanism of graphene oxide to EPFRs has been carried out in our previous research. The research on the chemical reaction of the generation mechanism of graphene oxide to EPFRs has been carried out in our previous research. In that study, we conducted high-temperature treatment experiments on actual atmospheric samples and glucose, and performed EPR, OC/EC and FT-IR tests on the processed samples. The experimental results show that the processed sample can generate EPFRs and is rich in benzene ring structure (benzene ring C=C) and heteroatom functional groups. Its EPR spectrum and *g*-factor are similar to graphene oxide.

- Chen, Q., Sun, H., Wang, M., Mu, Z., Wang, Y., Li, Y., Wang, Y., Zhang, L., Zhang, Z., 2018. Dominant fraction of EPFRs from Nonsolvent-Extractable organic matter in fine particulates over Xi'an, China. Environ. Sci. Technol. 52 (17), 9646−9655.

(9) Lines 243-314: These paragraphs have the problems as the discussion of g-factors. Everything is mixed together, with sentences that are hard to follow. I suggest really trying to reorganize this so that it is easier to follow.

We appreciate this comment from the reviewer. We have rewritten this part.

L252-300 “As shown in Figure 3a1, the typical spectral characteristic of summer factor 1 is that it contains a small fraction of EC components and a large amount of OC components, which indicates that combustion may be the source associated with this factor. This factor has the highest loading of OC, especially WISOC; this fraction mainly contains macromolecular organic substances, which are considered to contribute to the main atmospheric particulate EPFRs and to be graphite oxide-like substances (Chen et al., 2017; Chen et al., 2018a). Factor 2 is different from factor 1; factor 2 is more likely the combustion of fossil fuels, while factor 1 should be other combustion sources instead of burning coal, such as biomass combustion. The generation process is similar to a hybrid process, which includes the graphite oxide-like substances produced by incomplete combustion and the EPFRs formed by some metal oxides. The typical characteristic of factor 3 is that the contribution of metal elements is relatively high, while the contributions of EC and OC are very low. Metal elements such as Al, Ti, Mn, and Co are typical crust elements, so this factor may represent dust sources (Pan et al., 2013; Srivastava et al., 2007; Trapp et al., 2010). The generation process of EPFRs. The others are likely derived from the electroplating metallurgy industry (detailed in S1). As shown in Figure 3a2, the contribution ratios of different factors show that the contribution ratios of factor 1 and factor 2 are the highest, and factor 3 has only a small contribution, which indicates that combustion sources, especially incomplete combustion, are the main sources of EPFRs. The particle size distribution characteristics show that factor 1 is mainly distributed in particles larger than 2.1 μm, while factor 2 is mainly distributed in particles smaller than 0.43 μm.

The results of the factor analysis in winter are different from those in summer. As shown in Figure 3b1, the typical spectral characteristic of factor 1 is that it contains a large amount of OC components and As and Se. As and Se are trace elements of coal combustion, as shown in many studies (Pan et al., 2013; Tian et al., 2010), so coal combustion may be the source represented by this factor. From the generation process viewpoint, the factor does not contain EC, but the content of OC is very high. In the particles with a particle size of less than 3.3, which is mainly present in factor 1, the concentration of OC is 16 times that of EC. So it may be mainly a graphite oxide-like substance formed by the agglomeration of gaseous volatile organic compounds (VOCs) generated during combustion. The typical spectral characteristics of factor 2 are due to a large amount of V and some Al, EC and OC. OC and EC are also typical combustion products. V is rich in fossil fuels, especially fuel oil (Karnae et al., 2011). Therefore, traffic is the source represented by this factor. The factor contains crust elements such as Al and Mn, so it is speculated that this factor may also include traffic-related dust. The typical spectral characteristics of factor 3 are similar to those of factor 1, and both contain relatively large amounts of As and Se, with the exception that factor 3 contains a large amount of EC, indicating that it is also mainly derived from incomplete combustion sources. The generation process of factor 3 should be different from factor 1, which may include both the graphite oxide-like

material generated by fuel coking and the EPFRs generated by the metal oxide. The other factors are mainly atmospheric dust and electroplating or metallurgy (see text S1). As shown in Figure 3b2, factor 1 and factor 2 have the highest proportions, and factor 3 also has a small contribution, which indicates that winter is the same as summer, and combustion sources are the main source of EPFRs. The particle size distribution characteristics show that factor 1 is mainly distributed in particles with a size of 0.43 - 3.3 μm, while factor 2 is mainly distributed in particles lager than 3.3 μm."

(10) Line 339: I believe this should be Gehling and Dellinger, (2013).

We appreciate this comment from the reviewer. We have corrected this mistake.

(11) Lines 402-403: This sentence is backwards, the trachea and alveoli are exposed to EPFRs not the other way around.

We appreciate this comment from the reviewer. We have corrected this mistake as follows:

L393-394: The trachea and alveoli are also exposed to EPFRs, and the risk of exposure is equivalent to that of 8 cigarettes per person per day.

(12) It is hard to distinguish the blue and green colors in the (a) panels of Figures 1 and 2. Please choose better colors.

We appreciate this comment from the reviewer. We have changed the colors in panel (a) of Figures 1 and 2 to green and red as follows:

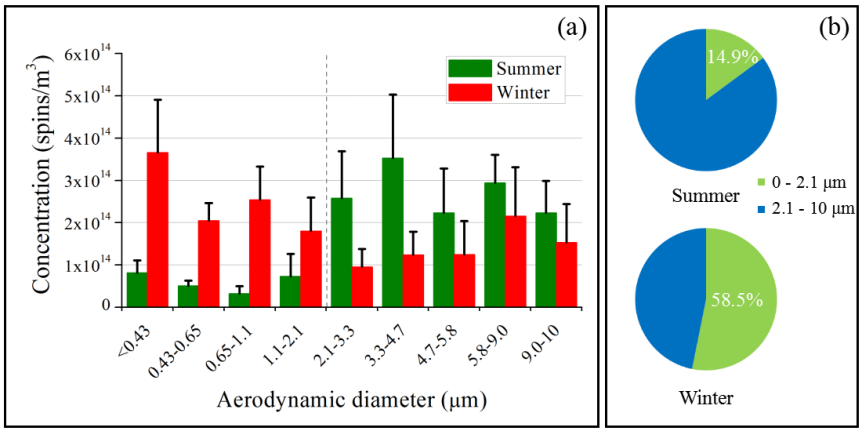

Figure 1. The concentration of EPFRs in PM with different particle sizes. (a) Atmospheric concentrations of EPFRs in different particle sizes in summer and winter. (b) The relative contribution of fine particles and coarse particles to the total EPFR concentration.

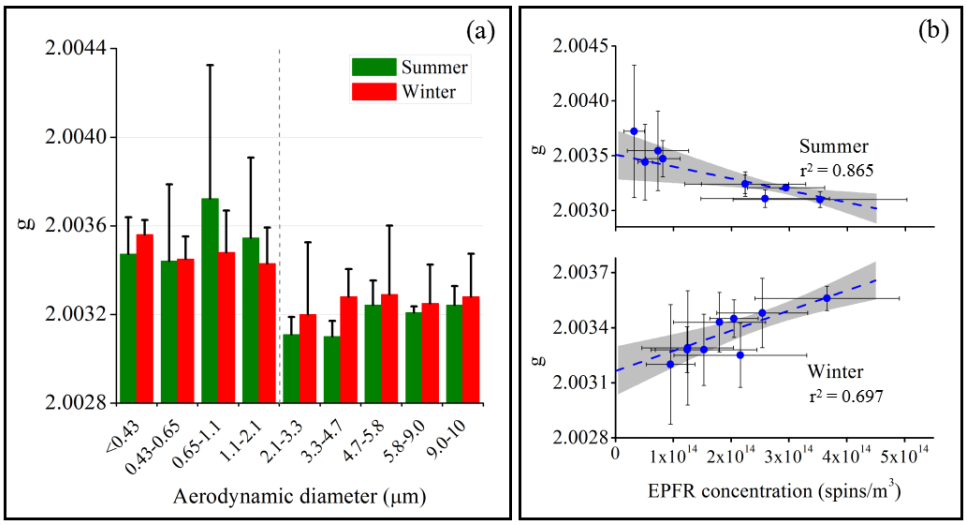

Figure 2. A *g*-factor comparison. (a) Comparison of *g*-factors of EPFRs in different particle sizes in different seasons. (b) Correlation analysis of *g*-factors and concentrations of EPFRs in summer and winter PM. The gray areas in the figure represent 95% confidence intervals.

(13) Supplement In the fifirst paragraph there is superscript 3 – is this supposed to be a reference? Figure S7 - the caption and axis – 'modle' should be 'model'.

We appreciate this comment from the reviewer. The superscript 3 in the supplementary information is an error and has been deleted. We have modified Figure S7 as follows:

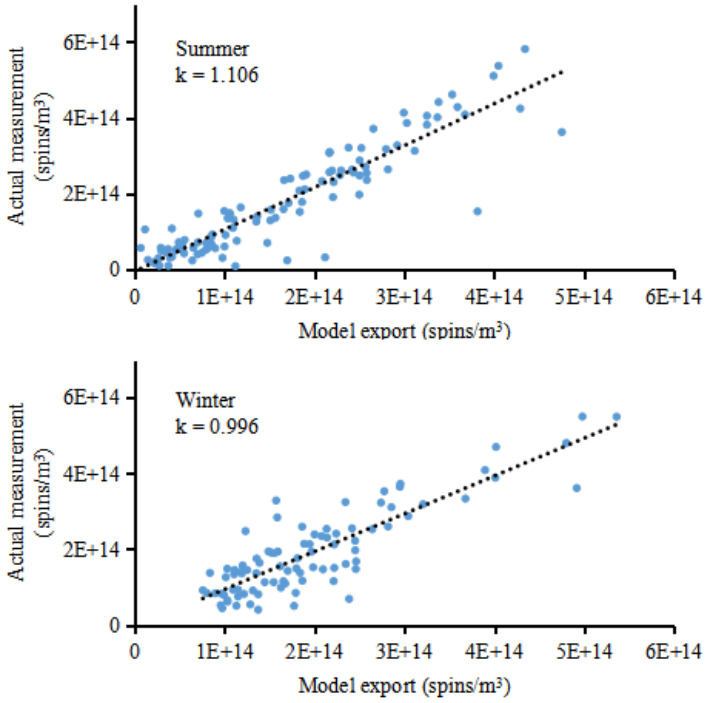

Figure S7. Comparison of the concentration of modle export and actual measurement.

Size-resolved exposure risk of persistent free radicals (PFRs) in atmospheric aerosols and their potential sources

Qingcai Chen,[a,] Haoyao Sun,[a,] Wenhuai Song,[b] Fang Cao,[b] Chongguo Tian,[c] Yan-Lin Zhang[b*]

[a] *School of Environmental Science and Engineering, Shaanxi University of Science and Technology, Xi'an 710021, China*

[b] *Yale–NUIST Center on Atmospheric Environment, International Joint Laboratory on Climate and Environment Change (ILCEC), Nanjing University of Information Science and Technology, Nanjing 210044, China*

[c] *Key Laboratory of Coastal Environmental Processes and Ecological Remediation, Yantai Institute of Coastal Zone Research, Chinese Academy of Sciences, Yantai, 264003, China*

[*]Corresponding Author at: Ningliu Road 219, Nanjing 210044, China.

E-mail address: dryanlinzhang@outlook.com or zhangyanlin@nuist.edu.cn (Yan-Lin Zhang).

Abstract: Environmentally persistent free radicals (EPFRs) are a new type of substance with potential health risks. EPFRs are widely present in atmospheric particulates, but there is a limited understanding of the size-resolved health risks of these radicals. This study ~~first reported~~reports the exposure risks and source of EPFRs in atmospheric particulate matter (PM) of different particle sizes (<10 μm) in Linfen, a typical coal-burning city in China. The type of EPFRs in fine particles (< 2.1 μm) is different from that in coarse particles (2.1-10 μm) in both winter and summer. However, the EPFR concentration is higher in coarse particles than in fine particles in summer, and the opposite trend is found in winter. In both seasons, combustion sources are the main sources of EPFRs with coal combustion as the major contributor in winter, while ~~biomass combustion is~~other fuel combustions are the major source in summer. Dust contributes part of the EPFRs and it is mainly present in coarse particles in winter and the opposite in summer. The upper respiratory tract was found to be the area with the highest risk of exposure to EPFRs of the studied aerosols, with an exposure equivalent to that of approximately 21 cigarettes per person per day. Alveolar exposure to EPFRs is equivalent to 8 cigarettes per person per day, with combustion sources contributing the most to EPFRs in the alveoli. This study helps us to better understand the potential health risks of atmospheric PM with different particle sizes.

Key words: EPFRs; particle size distribution; source; generation ~~mechanism~~process

35 **TOC Art:**

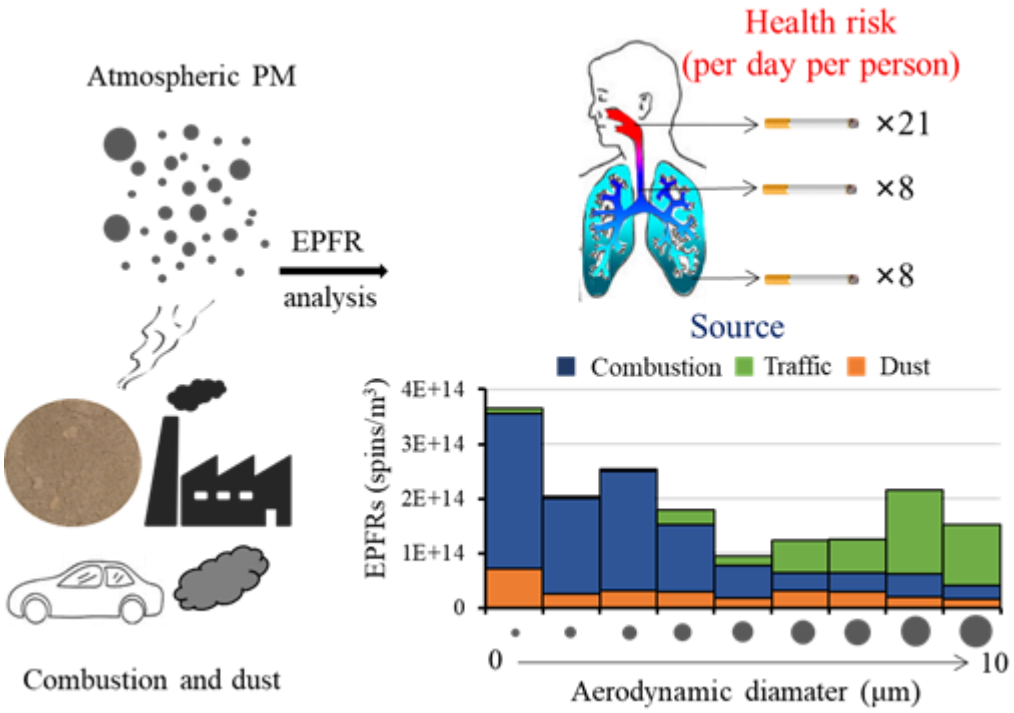
Atmospheric PM
EPFR
analysis
Combustion and dust
Health risk
(per day per person)
×21
×8
×8
Source
Combustion
Traffic
Dust
EPFRs (spins/m³)
4E+14
3E+14
2E+14
1E+14
0
0
10
Aerodynamic diamater (μm)

36

1. Introduction

Free radicals are atoms or groups containing unpaired electrons, such as hydroxyl radicals and superoxide radicals, and they usually have strong chemical reactivity and short lifetimes (Pryor et al., 1986; Finkelstein., 1982). Free radicals with long lifetimes (months or even years) in the environment are currently called environmentally persistent free radicals (EPFRs), which have received much attention in recent years as new environmentally hazardous substances (Vejerano et al., 2018; Gehling, 2013; Chen et al., 2019c). EPFRs can be used as an active intermediate to catalyze the production of reactive oxygen species (ROS) by oxygen molecules, thus endangering human health (D'Arienzo et al., 2017; Thevenot et al., 2013; Harmon et al., 2018; Blakley et al., 2001; Khachatryan et al., 2011). Studies have found that EPFRs are present in different environmental media, such as water and soil, and even in the atmosphere (Dellinger et al., 2001; Truong et al., 2010; Vejerano et al., 2012).

A number of studies have investigated the occurrences, sources and formation ~~mechanisms~~process of EPFRs in atmospheric particulates in different regions. For example, in the studies of Rostock in Germany, Taif in Saudi Arabia and Xuanwei in China, the average concentration of EPFRs in atmospheric particulate matter (PM) was reported to be in the range of ~ 10^{16} - 10^{18} spins/g (Wang et al., 2018; Arangio et al., 2016; Shaltout et al., 2015). Atmospheric EPFRs are mainly carbon-centered radicals with adjacent oxygen atoms (Gehling et al., 2013). EPFRs of different lifetimes are present in atmospheric PM, with only a few hours for short-lifetime EPFRs and several years for long-lifetime EPFRs that show no signs of decay (Gehling et al., 2013; Chen et al., 2019c). Most studies indicate that sources of transportation and combustion may be the primary EPFR sources in atmospheric PM (Wang et al., 2018; Yang et al., 2017; Chen et al., 2019b). Chen et al. (2018b and 2019b) found that strong atmospheric photochemical effects in summer and dust particles may also be important sources of EPFRs. The process of electron transfer and stabilization between the surface of metal oxides (such as iron, copper, zinc and

nickel) and substituted aromatic molecules under high temperatures is considered to be the main ~~mechanism~~process for the formation of EPFRs in atmospheric particles (Truong., 2010; Vejerano et al., 2012a; Patterson et al., 2013; Vejerano., 2010; Vejerano et al., 2012b). However, the study by Chen et al. (2018a) suggests that EPFRs in atmospheric particulates are mainly derived from graphite oxide-like substances produced during combustion. In addition to primary sources such as combustion, secondary chemical processes in the atmosphere may also be an important source of EPFRs in atmospheric PM (Chen et al. 2019b and 2019d; Tong et al., 2018).

Different particle sizes of atmospheric PM pose different health risks to humans, depending on the deposition efficiency of the particles and the chemical composition and concentrations of hazardous substances they contain (Strak et al., 2012; Valavanidis et al., 2008). Among various hazardous substances, EPFRs may also be involved in the toxicity of atmospheric particulates. Yang et al. (2017) studied the the EPFRs that are extractable by dichloromethane in different particle sizes in Beijing in winter and found that the concentration of EPFRs was the highest in particles with sizes < 1 μm. Arangio et al. (2016) found that the concentration of EPFRs in 180 nm particles was the highest in the 56 nm - 1.8 μm particle size range. Although several studies have examined the particle size distribution of EPFRs, systematic studies have not been conducted on the formation ~~mechanism~~process, source and exposure assessment of EPFRs in atmospheric particles with different particle sizes.

This study takes Linfen as an example. Linfen is one of the cities in China with the most serious air pollution and is a typical coal-burning city. The particle size distribution of EPFRs in atmospheric PM in this region was studied by EPR spectrometry. The effects of particle size and season on the source, formation ~~mechanism~~process, and health risk of EPFRs were revealed. In particular, the comprehensive health risks of EPFRs were evaluated, and it was found that the upper respiratory tract is the area with the highest risk of EPFRs exposure, which is equivalent to twenty-one cigarettes per person per day. This study is of great

significance for understanding the source and formation ~~mechanism~~process of EPFRs in atmospheric particulates as well as for health risk assessments.

2. Experimental section

2.1 Sample collection

The sampling site for this study is located in Hongdong (36°23', 111°40'E) in Shanxi, China. To collect atmospheric particles of different sizes (0-10 μm), this study used a Thermo-Anderson Mark II sampler to collect aerosol samples of 9 sizes. The samples were collected on a prebaked quartz filter (450 °C, 4.5 hours), and the sampling dates were as follows: in winter, January 26 to February 4, 2017, n = 10; and in summer, July 31 to August 24, 2017, n = 12. The samples were placed in a -20 °C refrigerator prior to analysis.

2.2 EPFR analysis

The EPR spectrometer (MS5000, Freiberg, Germany) is used to detect EPFRs in atmospheric samples. Cut the ~~Specific testing protocols have been described previously (Chen et al., 2018c. The~~ sample filter ~~was cut~~ into thin strips (5 mm × 28 mm), and ~~clamped with a~~put it into the sample tank of the quartz ~~piece, and then~~tissue cell (the size of the sample tank is 10 mm × 30 mm)., Then the quartz ~~piece~~tissue cell with attached filter sample was placed in a resonant cavity and analyzed by an EPR spectrometer ~~(MS5000, Freiberg, Germany).~~ The detection parameters were magnetic field strength, 335 - 342 mT; detection time, 60 s; modulation amplitude, 0.20 mT; number of detections, 1; and microwave intensity, 8.0 mW. Specific testing protocols have been described previously (Chen et al., 2018c).

2.3 Carbon composition analysis

The contents of organic carbon (OC) and elemental carbon (EC) in the filter samples were analyzed using a semicontinuous OC/EC analyzer (Model 4, Sunset Lab. Inc., Oregon, USA) with a NIOSH 5040 detection protocol (Lin et al., 2009).

The water-soluble organic carbon (WSOC) concentration was analyzed using an automatic TOC-LCPH analyzer (Shimadzu, Japan). The WSOC extraction was performed with ultrapure water under ultrasonication for 15 minutes, and all WSOC concentrations were blank corrected. The concentration of OC in the MSM (Methanol-soluble materials) was calculated as the difference between the OC and WSOC (Water-soluble organic carbon) concentrations. This calculation assumes that all water-insoluble organic carbon (WISOC) in the aerosol can be extracted with MeOH, and the rationality of this assumption has been verified elsewhere (Mihara et al., 2011; Liu et al., 2013; Cheng et al., 2016; Chen et al., 2019a).

2.4 PAH analysis

PAHs were detected using gas chromatography/mass spectrometry (GC/MS) on a GC7890B/MS5977A (Agilent Technologies, Clara, CA~~), as described in detail in a previously published study (Han et al.,~~). Quartz-fiber filter samples (8 mm in diameter) were cut from each 25-mm quartz-fiber filter substrates used on the ELPI impactor stages using a stainless-steel round punch over a clean glass dish and loaded into the TD glass tube. Next, the TD glass tube was heated to 310 °C at a rate of 12 °C/min and thermally desorbed at 310 °C for 3 min. The desorbed organic compounds were trapped on the head of a GC-column (DB-5MS: 5% diphenyl-95% dimethyl siloxane copolymer stationary phase, 0.25-mm i.d., 30-m length, and 0.25-mm thickness). Sixteen target PAHs were identified based on retention time and qualified ions of the standards, including 16 EPA parent PAHs (p-PAHs). The method detection limits (MDLs) ranged from 0.2 pg/mm2 (Ace) to 0.6 pg/mm2 (Incdp). Naphthalene-D8, acenaphthene-D10, phenanthrene-D10, chrysene-D12, and perylene D12 were used for the analytical recovery check. All compounds were recovered with a desorption recovery percentage of > 90%. Specific testing protocols have been described previously (Han et al., 2018).

2.5 Metal element analysis

The concentration of metal elements in the samples was determined by a Thermo

X2 series inductively coupled plasma mass spectrometer (ICP-MS, Thermo, USA). The metal elements analyzed in summer were Na, Mg, K, Ca, Ti, V, Cr, Mn, Fe, Co, Ni, Cu, Zn, As, Cd, Pb, and Al, and those in winter were Al, Zn, V, Cr, Mn, Co, Ni, Cu, As, Se, Sr, Cd, Ba, and Pb. The specific measurement method is based on the study of Qi et al (2016).

2.6. Data statistics method

The source and formation ~~mechanism~~process of EPFRs in PM with different particle sizes were analyzed by nonnegative matrix factorization (NMF). The method is based on the study of Chen et al (2016 and 2019e). Briefly, NMF analysis of EPFR data, metal element contents, OC/EC contents and PAH contents was performed in MATLAB. The version of the NMF toolbox is 1.4 (https://sites.google.com/site/nmftool/). ~~First, a~~Use the gradient-based multiplication algorithm ~~is used~~ to find a solution from multiple random starting values, and then use the first algorithm ~~is used~~ to find ~~a solution to~~ the final solution ~~using a~~based on the least squares effective set algorithm. To find a global solution, the model was run 100 times, each time with a different initial value. By comparing the 1-12 factor model (Figure S4) with the residual of the spectral load, the 6 factor (summer) and 10 factor (winter) NMF models were finally selected.

2.7. EPFR exposure evaluation

To assess the health risks of EPFRs, ~~we~~this study divided the respiratory system into three parts based on the human breathing model: extrathoracic (ET) areas, including the anterior nasal cavity, posterior nasal cavity, oral cavity, and throat; tracheobronchial (TB) areas, including the trachea, bronchi, bronchioles, and terminal bronchi; and pulmonary (P) areas, including the alveolar ducts and alveoli. Then, the sedimentation rates of different particle sizes in different areas of the respiratory system were determined to calculate the exposure risk of EPFRs. Here, the human respiratory system particulate deposition model of Salma et al. (2002) was used, and the specific data can be found in Table S3 and S4.

In addition, ~~we converted~~ the daily inhaled concentration of EPFRs into the concentration of free radicals in cigarettes were converted. The specific conversion method is as follows:

$$N_{cig} = (C_{EPFRs} \cdot V)/(RC_{cig} \cdot C_{tar}) \quad (1)$$

where N_{cig} represents the number of cigarettes (/person/day), C_{EPFRs} (spins/m^3) represents the atmospheric concentration of EPFRs in PM, and V represents the amount of air inhaled by an adult per day (20 m^3/day) (Environmental Protection Agency, 1988). RC_{cig} (4.75×10^{16} spins/g) (Baum et al., 2003; Blakley et al., 2001; Pryor et al., 1983; Valavanidis and Haralambous, 2001) indicates the concentration of free radicals in cigarette tar, and C_{tar} (0.013 g/cig) indicates the amount of tar per cigarette (Gehling et al., 2013).

3. Results and discussion

3.1 Concentrations and types of EPFRs

Figure 1a shows the concentration distribution of EPFRs with different particle sizes in different seasons. EPFRs were detected in the particles of each tested size (the EPR spectrum is shown in Figure S1), but their EPFR concentration levels were different. In summer, the concentration of EPFRs in fine particles (particle size < 2.1 μm) is (3.2 - 8.1) × 10^{13} spins/m^3, while the concentration of EPFRs in coarse particles (particle size > 2.1 μm) is 1-2 orders of magnitude higher than that of fine particles, reaching values of (2.2 - 3.5) × 10^{14} spins/m^3. Winter samples show completely different characteristics from summer samples. The concentration of EPFRs in fine particles (particle size < 2.1 μm) is (1.8 - 3.6) × 10^{14} spins/m^3, while the concentration of EPFRs in coarse particles (particle size > 2.1 μm) is smaller than that of fine particles, with values of (1.0 - 2.1) × 10^{14} spins/m^3. In addition, the concentration of EPFRs in particulates <0.43 μm in winter is very high, but it is very low in summer. ~~This~~According to the results of factor analysis in part 3.2 of this study, this particulate matter is related to combustion, which indicates that coal combustion

in winter may provide an important contribution to EPFRs. The EPFR concentration in the fine PM of Linfen reported above is equivalent to that in the fine PM of Xi'an, but it is ten times smaller than that in the fine PM of Beijing (Yang et al., 2017; Chen et al., 2019b). Although the particle size distribution characteristics of EPFRs in winter and summer are different, their concentration levels are similar, which indicates that the EPFR concentration is not related to the PM concentration, but is determined by the source characteristics. The source characteristics will be discussed in detail in the factor analysis section.

Figure 1b shows the size-segregated contribution of ~~the~~ EPFR concentration to the overall ~~EPFR concentration in coarse and fine particles.~~. The contribution of fine PM in summer is only 14.9%, while ~~that of fine PM~~ in winter is 58.5%. The differences in EPFR concentrations with particle size may be related to the source of EPFRs. For example, coarse particles are often associated with dust sources~~.~~ and biogenic aerosols. In another study, ~~we~~the results have shown that dust particles contain large amounts of metallic EPFRs and that they can be transported over long distances (Chen et al., 2018b). EPFRs in fine particles may be mainly derived from the combustion process, such as traffic sources, which are considered to be an important source of EPFRs in atmospheric PM (Secrest et al., 2016; Chen et al., 2019b). Due to winter heating in the Linfen area, the amount of coal burning increases sharply in this season. In 2017, the nonclean heating (Coal-fired heating) rate of urban heating energy structures in Linfen was 40% (data source: http://www.linfen.gov.cn/). With the burning of coal, large amounts of EPFRs are produced, and in the summer, EPFRs emitted by burning coal should be much less than those emitted in winter. This can explain to a certain extent that the contribution of fine particles to summer EPFRs is small, and the contribution of winter EPFRs is very large.

The *g*-factor obtained by using EPR to detect the sample is ~~a~~an important parameter ~~used~~ to distinguish the type of EPFR. It is the ratio of the electronic magnetic moment to its angular momentum (Shaltout et al., 2015; Arangio et al., 2016). The *g*-factor of carbon-centered persistent free radicals is generally less than 2.003, the *g*-factor of

oxygen-centered persistent radicals is generally greater than 2.004, and the g factor of carbon-centered radicals with adjacent oxygen atoms is between 2.003 and 2.004 (Cruz et al., 2012). Figure 2a shows the *g*-factor distribution characteristics of EPFRs in different particle sizes in summer and winter. The *g*-factor of fine particles and coarse particles ~~also~~ shows different characteristics. The *g*-factor of EPFRs in fine particles (particle size < 2.1 μm) ranges from 2.0034 to 2.0037, which may be from carbon-centered radicals with adjacent oxygen atoms. However, the *g*-factor of EPFRs in coarse particles (particle size > 2.1 μm) is significantly less than that of fine particles. The *g*-factor ranges from 2.0031 to 2.0033, indicating that EPFRs in coarse particles are more carbon-centered than those in fine particles and are free of heteroatoms. ~~Although the particle size characteristics of the *g*-factor of the EPFRs in summer and winter are the same, the~~As shown in Figure 2b, the variation in the *g*-factor with concentration in different season is different. ~~As shown in Figure 2b, the~~The *g*-factor of summer PM showed a significant decreasing trend with increasing concentration, while the *g*-factor of winter PM showed a significant increasing trend with increasing EPFR concentration. Oyana et al. (2017) studied EPFRs in the surface dust of leaves in the Memphis region of the United States and found that the concentration of EPFRs was positively correlated with the *g*-factor, and they believed that this was related to the source of EPFRs. This phenomenon indicates that the sources and toxicity of EPFRs in winter and summer are different. ~~Figure 1 shows that the summer EPFRs are mainly derived from coarse particles, while the *g*-factor of EPFRs in coarse particles is smaller than that in fine particles, so the *g*-factor of EPFRs in summer decreases with an increase in EPFR concentration. In winter, fine particles contribute more to EPFRs, so the *g*-factor of EPFRs in winter increases with the concentration of EPFRs.~~

3.2 Factor Analysis of EPFRs

To explore the possible sources and formation ~~mechanism~~process of EPFRs in atmospheric particles with different particle sizes, the NMF model was used to statistically analyze EPFRs, carbon components, PAHs and metal elements in samples.

The factors obtained by the NMF model should reflect the different sources ~~mechanisms~~and generation process of EPFRs. As shown in Figure 3a1 and b1, the three main contributing factors to EPFRs in summer and winter are shown (see Figure S5, S6 for spectra of other factors), which explain 94.5% and 83.8% of the EPFR concentrations in summer and winter, respectively.

As shown in Figure ~~3a~~3a1, the typical spectral characteristic of summer factor 1 is that it contains a small fraction of EC components and a large amount of OC components, which indicates that combustion may be the source associated with this factor. This factor has the highest loading of OC, especially WISOC; this fraction mainly contains macromolecular organic substances, which are considered to contribute to the main atmospheric particulate EPFRs and to be graphite oxide-like substances (Chen et al., 2017; Chen et al., 2018a). ~~The result shows that factor 1 has the highest contribution of all the factors to EPFRs in PM (69.6%), and they are mainly distributed in particles with sizes > 2.1 μm. Factor 2 is typically characterized by a high contribution from EC and a small fraction of OC and metal elements, which is a typical source of incomplete combustion.~~ Factor 2 is different from factor 1; factor 2 is more likely the combustion of fossil fuels, while factor 1 ~~may~~should be other combustion sources instead of burning coal, such as biomass combustion ~~source~~. The generation ~~mechanism~~process is similar to a hybrid ~~mechanism~~process, which includes the graphite oxide-like substances produced by incomplete combustion and the EPFRs formed by some metal oxides. ~~The relative contribution of these EPFRs is 13.5% and is mainly distributed in particles with a size < 0.43 μm.~~ The typical characteristic of factor 3 is that the contribution of metal elements is relatively high, while the contributions of EC and OC are very low. Metal elements such as Al, Ti, Mn, and Co are typical crust elements, so this factor may represent dust sources (Pan et al., 2013; Srivastava et al., 2007; Trapp et al., 2010). The generation ~~mechanism may be mainly due to the participation of metal oxides in the generation~~process of EPFRs. ~~Compared with the other factors, this factor also has a partial load on PAHs, indicating that PAHs may be involved in the formation of metal oxide-related EPFRs.~~

~~These EPFRs have a relatively low contribution to total EPFRs (approximately 12.4%) and are mainly distributed in particles with a size of 0.43 - 2.1 μm.~~ The ~~EPFR contribution of other factors is 4.4%; they~~others are likely derived from the electroplating metallurgy industry (detailed in S1). As shown in Figure 3a2, the contribution ratios of different factors show that the contribution ratios of factor 1 and factor 2 are the highest, and factor 3 has only a small contribution, which indicates that combustion sources, especially incomplete combustion, are the main sources of EPFRs. The particle size distribution characteristics show that factor 1 is mainly distributed in particles larger than 2.1 μm, while factor 2 is mainly distributed in particles smaller than 0.43 μm.

The results of the factor analysis in winter are different from those in summer. As shown in Figure ~~3b~~3b1, the typical spectral characteristic of factor 1 is that it contains a large amount of OC components and As and Se. As and Se are trace elements of coal combustion, as shown in many studies (Pan et al., 2013; Tian et al., 2010), so coal combustion may be the source represented by this factor. From the generation ~~mechanism~~process viewpoint, the factor does not contain EC, but the content of OC is very high. In the particles with a particle size of less than 3.3, which is mainly present in factor 1, the concentration of OC is 16 times that of EC. So it may be mainly a graphite oxide-like substance formed by the agglomeration of gaseous volatile organic compounds (VOCs) generated during combustion. ~~These EPFRs are mainly distributed in particles with a size of 0.43 - 3.3 μm, and their contribution to EPFRs in PM is up to 44.6%. Factor 2 contributes 25.7% to EPFRs.~~ The typical spectral characteristics of factor 2 are due to a large amount of V and some Al, EC and OC. OC and EC are also typical combustion products. V is rich in fossil fuels, especially fuel oil (Karnae et al., 2011). Therefore, traffic is the source represented by this factor. The factor contains crust elements such as Al and Mn, so it is speculated that this factor may also include traffic-related dust. ~~The particle size distribution shows that such EPFRs are mainly present in large particles with a size of 3.3 - 10 μm.~~ The typical spectral characteristics of factor 3 are similar to those of factor 1, and both

contain relatively large amounts of As and Se, with the exception that factor 3 contains a large amount of EC, indicating that it is also mainly derived from incomplete combustion sources. The generation ~~mechanism~~process of factor 3 should be different from factor 1, which may include both the graphite oxide-like material generated by fuel coking and the EPFRs generated by the metal oxide. ~~These EPFRs are mainly distributed in particles with a size of <0.43 μm, and their total contribution to EPFRs in PM is 13.4%. In addition, the~~ The other factors ~~contribute 16.3% to EPFRs, and these factors~~ are mainly atmospheric dust ~~(11.4%)~~ and electroplating or metallurgy (~~4.9%) (~~see text S1). ~~The results of this study~~As shown in Figure 3b2, factor ~~analysis were similar to the results of the study by Wang et al. (2019) on EPFRs in Xi'an. They found~~1 and factor 2 have the highest proportions, and factor 3 also has a small contribution, which indicates that ~~coal, traffic~~winter is the same as summer, and ~~dust were~~ combustion sources are the main ~~sources of EPFRs and accounted for 76.2% of the total~~ source of EPFRs. The particle size distribution characteristics show that factor 1 is mainly distributed in particles with a size of 0.43 - 3.3 μm, while factor 2 is mainly distributed in particles lager than 3.3 μm.

Based on the above analysis, it can be found that combustion sources are the main sources of EPFRs, and EPFRs from these sources are mainly graphite oxide-like substances generated by the polymerization of organic matter or fuel coking. Studies have shown that graphene oxide can cause cell damage by generating ROS (Seabra et al., 2014). The surface of these compounds contains not only carbon atoms but also some heteroatoms, which leads to disorder and the presence of defects in the carbon-based structure (Lyu et al., 2018; Chen et al., 2017a; Mukome et al., 2013; Keiluweit et al., 2010). The dust source is also a source of important EPFRs identified in this study (with a contribution of approximately 10%). It was shown in the above analysis that the concentration of EPFRs in coarse particles has a significant correlation with the concentration of metallic elements, particularly crustal elements. Some crustal elements, such as Al, and Fe, not only have their own paramagnetism (Li et al., 2017; Yu et al., 2013; Nikitenko et al., 1992), but also interact with aromatic

compounds attached to the surface of the particles to produce a stable single-electron structure.

3.3 *Health risk of EPFRs*

To evaluate the health risks of EPFRs in PM with different particle sizes, ~~we~~this study evaluated the comprehensive exposure of EPFRs based on the deposition efficiency of PM with different particle sizes in different parts of the human body. The results are shown in Figure 4a. The ET region is the region with the highest EPFR exposure, while the TB and P regions have relatively close EPFRs. This result shows that atmospheric EPFRs are the most harmful to the health of the human upper respiratory tract. Comparing the EPFR exposure in different seasons indicates that the exposure risk in the ET area in summer is significantly higher than that in winter. This difference occurs because the concentration of EPFRs in coarse particles is much higher than that of fine particles in summer and the deposition efficiency of large particles in the ET area is generally higher. Fine particles are more efficiently deposited in the P region, leading to a higher risk of EPFR exposure in the P region in winter.

EPFRs were ~~first~~ found early in cigarette tar and are considered one of the health risk factors in cigarette smoke (Lyons et al., 1960); thus, in this study, the exposure risks of EPFRs in particles deposited in the human body were converted to the equivalent number of cigarettes inhaled per adult per day. As shown in Figure 4b, the ET area is the most contaminated area, with an average equivalence of twenty-one cigarettes (twenty-five in summer and sixteen in winter). The average values for the TB area (nine in summer and seven in winter) and P area (seven in summer and ten in winter) are eight. The results indicate that EPFRs pose significant health risks to human lungs in both winter and summer. Other similar studies, such as a study of the average amount of EPFRs in $PM_{2.5}$ inhaled per person per day in Xi'an in 2017, found values equivalent to approximately 5 cigarettes (Chen et al., 2018a). Gehring ~~et al.~~and Dellinger (2013) found that EPFR exposure in $PM_{2.5}$ is equivalent to approximately 0.3 cigarettes per person per day in St. Joaquin County, the location with the worst air

pollution in the United States. The average exposure risk of EPFRs in fine particles in the Linfen area (approximately 13 cigarettes) was higher than those in these two studies. However, these previous studies only studied the exposure risk of EPFRs in fine particles. The results of this study indicate that the health risks of EPFRs are significantly increased when the particle size distribution of EPFRs is taken into account. Therefore, it is important to study the source characteristics and generation ~~mechanism~~process of EPFRs with different particle sizes, which will be discussed in detail in the following sections.

This study calculated the proportion of EPFRs with different particle sizes in different parts of the respiratory system based on the deposition efficiency of particles with different particle sizes. As shown in Figure 4c, in the ET region and the TB region, coarse particles are the dominant component in summer and winter. In particular, in summer, the proportion of EPFRs in coarse particles in these two regions exceeds 95%. In the P region, there are significant differences between summer and winter. The P region in summer is still dominated by coarse particles, but its proportion is significantly lower than those in the ET and TB regions. In the P region in winter, fine particles are the dominant component (approximately 70%). These distribution characteristics indicate different sources of EPFRs in different regions. As shown in Figure 4d, in summer, combustion sources are the main source of EPFRs in the respiratory system. In winter, combustion and transportation sources contribute equally in the EP and ET regions, while in the alveoli, combustion sources are the main contributor. The ET region is the area with the highest risk of exposure to EPFRs (21 cigarettes). The generation ~~mechanism~~process of these EPFRs is mainly attributable to graphene oxide-like substances. Studies have shown that graphene oxide is cytotoxic (Harmon et al., 2018). In the alveoli, the contribution of combustion sources is significantly increased (especially in winter). These EPFRs are mainly generated by the action of metal oxides and organic substances. Studies have shown that such EPFRs can generate ROS in the lung fluid environment (Khachatryan et al., 2011). ~~Therefore, the health risks of EPFRs from different sources and~~

~~mechanisms should be evaluated in the future in order to better assess the harm caused by EPFRs to the body.~~

4. **Conclusions and environmental implications**

This study systematically reported the particle size distribution of EPFRs in atmospheric PM in Linfen, which is one of the most polluted cities in China and is located in a typical coal-burning area. In addition, this study evaluated the comprehensive health risks of EPFRs, and reported possible sources and formation ~~mechanisms~~process of atmospheric EPFRs with respect to different particle sizes. The following main conclusions were obtained.

(1) This study found that EPFRs are widely present in atmospheric particles of different particle sizes and exhibit significant particle size distribution characteristics. ~~EPFR concentrations are higher in coarse particles than in fine particles in summer and vice versa in winter. Differences were also found in the g-factors of EPFRs in coarse particles and fine particles, indicating that the types of EPFRs of different particle sizes were also different.~~ The results of this study demonstrate that the concentrations and types of EPFRs are dependent on particle size and season. ~~This result~~This seasonal characteristic of EPFRs is mainly affected by the PM sources, this result also indicates that the potential toxicity caused by EPFRs may also vary with particle size and season.

(2) This study reported the possible source and formation ~~mechanisms~~process of atmospheric EPFRs in different particle sizes. The results show that combustion is the most important source of EPFRs (>70%) in both winter and summer PM samples in Linfen. ~~Atmospheric dust also contributes to EPFRs (~10%), and they are mainly found in fine particles in summer and coarse particles in winter.~~ The graphite oxide-like ~~mechanism~~process has the highest contribution (~70%) and is mainly distributed in particles with a size of > 0.43 μm~~, while EPFRs in which metal oxides participate are mainly distributed in particles with a size of < 0.43 μm.~~. These findings deepen our understanding of the pollution characteristics of atmospheric EPFRs and

are useful for controlling EPFR generation in heavily polluted areas.

(3) This study assessed the exposure risk of EPFRs in different areas of the respiratory system. The results show that the upper respiratory tract is the area with the highest EPFR exposure ~~(the value in summer is higher than that in winter), with a value equivalent to 21 cigarettes per person per day. EPFRs are equally exposed to the trachea and alveoli~~. The trachea and alveoli are also exposed to EPFRs, and the risk of exposure is equivalent to that of 8 cigarettes per person per day. Coarse particles are the main source of EPFRs in the upper respiratory tract, while fine particles are mainly involved in the alveoli. ~~In summer, combustion sources are the main source of EPFRs in various parts of the respiratory system. In winter, traffic and other combustion sources are the main source of EPFRs in the upper respiratory tract, and combustion sources mainly contribute to the EPFRs in the alveoli.~~

Through this study, ~~we~~the results have shown that there are significant differences in the concentrations and types of EPFRs in particles of different sizes and these differences are due to the influence of the source and generation ~~mechanism~~process. In the future, assessments of the particle size distribution and the seasonality of EPFRs in atmospheric PM should be considered. Health risks are another focus of this study. ~~We~~It is found that the upper respiratory tract is the key exposure area of EPFRs, and the traffic source is the main source of EPFRs in this area. This finding is significant for a systematic assessment of the health risks of EPFRs. In view of the complexity and diversity of the formation ~~mechanisms~~process of EPFRs in actual atmospheric particulates, the relative contributions of EPFRs generated by different ~~mechanisms~~process and their associated health risks should be more comprehensively studied in the future.

Acknowledgments

This work was supported by the National Natural Science Foundation of China (grant numbers: 41877354, 41761144056 and 41703102), the Provincial Natural Science Foundation of Jiangsu grant no. BK20180040), the Natural Science

Foundation of Shaanxi Province, China (2018JM4011) and the fund of Jiangsu Innovation & Entrepreneurship Team.

Appendix A. Supplementary data

Appendix A contains additional details, including the EPR spectra of samples of different particle sizes, correlations between EPFRs and carbon in particles of different particle sizes, the results and errors of factor analysis, correlation analysis of EPFRs with metallic elements, and EPFR exposure in different areas of the human respiratory tract.

Code/Data availability: All data that support the findings of this study are available in this article and its Supplement or from the corresponding author on request.

Author contribution: Qingcai Chen: Research design, Methodology, Writing - Original Draft, Writing - Review & Editing, Project administration, Funding acquisition; Haoyao Sun: Investigation, Sample analysis, Writing - Original Draft, Writing - Review & Editing, Methodology, Formal analysis; Wenhuai Song: Investigation, Sample collection, Chemical analysis; Fang Cao: Investigation, Sample collection; Chongguo Tian: Investigation, Chemical analysis; Yan-Lin Zhang: Conceptualization, Writing - Review & Editing, Formal analysis, Validation, Funding acquisition.

Competing interests: The authors declare that they have no conflict of interest.

References

Arangio, A. M., Tong, H., Socorro, J., Pöschl, U., Shiraiwa, M., 2016. Quantification of environmentally persistent free radicals and reactive oxygen species in atmospheric aerosol particles. Atmos. Chem. Phys. 16 (20), 13105–13119.

Blakley, R. L., Henry, D. D., Smith, C. J., 2001. Lack of correlation between cigarette mainstream smoke particulate phase radicals and hydroquinone yield. Food. Chem. Toxicol. 39 (4), 401−406.

Baum, S.L., Anderson, I.G.M., Baker, R.R., Murphy, D.M., Rowlands, C.C., 2003. Electron spin resonance and spin trap investigation of free radicals in cigarette smoke: development of a quantification procedure. Anal. Chim. Acta 481, 1−13.

Cruz, A.L.N.D., Cook, R.L., Lomnicki, S.M., Dellinger, B., 2012. Effect of low temperature thermal treatment on soils contaminated with pentachlorophenol and environmentally persistent free radicals. Environ. Sci. Technol. 46, 5971−5978.

Chen, N., Huang, Y., Hou, X., Ai, Z., Zhang, L., 2017. Photochemistry of hydrochar: Reactive oxygen species generation and sulfadimidine degradation. Environ. Sci. Technol. 51 (19), 11278−11287.

Chen, Q., Mu. Z., Song, W., Wang, Y., Yang, Z., Zhang, L., Zhang, Y., 2019a. Size-resolved characterization of the chromophores in atmospheric particulate matter in Linfen, China. J. Geophys. Res-Atmos. 124, DIO: 10.1029/2019JD031149.

Chen, Q., Ikemori, F., Nakamura Y., Vodicka, P., Kawamura, K., Mochida, M., 2017. Structural and light-absorption characteristics of complex water-insoluble organic mixtures in urban submicron aerosols. Environ. Sci. Technol. 51(15), 8293−8303.

Chen, Q., Miyazaki, Y., Kawamura, K., Matsumoto, K., Coburn, S., Volkamer, R., Iwamoto, Y., Kagami, S., Deng, Y., Ogawa, S., 2016. Characterization of chromophoric water-soluble organic matter in urban, forest, and marine aerosols by HR-ToF-AMS analysis and excitation–emission matrix spectroscopy. Environ. Sci. Technol. 50 (19), 10351–10360.

Chen, Q., Sun, H., Mu, Z., Wang, Y., Li, Y., Zhang, L., Wang, M., Zhang, Z., 2019b. Characteristics of environmentally persistent free radicals in PM2.5: Concentrations, species and sources in Xi'an, Northwestern China. Environ. Pollut. 247, 18−26.

Chen, Q., Sun, H., Wang, J., Shan, M., Xue, J., Yang, X., Deng, M., Wang, Y., Zhang, L., 2019c. Long-life type — The dominant fraction of EPFRs in combustion sources and ambient fine particles in Xi'an. Atmos. Environ. 219, 117059.

Chen, Q., Sun, H., Wang, M., Mu, Z., Wang, Y., Li, Y., Wang, Y., Zhang, L., Zhang, Z., 2018a. Dominant fraction of EPFRs from Nonsolvent-Extractable organic matter in fine particulates over Xi'an, China. Environ. Sci. Technol. 52 (17), 9646−9655.

Chen, Q., Sun, H., Wang, M., Wang, Y., Zhang, L., Han, Y., 2019d. Environmentally persistent free radical (EPFR) formation by visible-light illumination of the organic matter in atmospheric particles. Environ. Sci. Technol, 53 (17), 10053−10061.

Chen, Q., Wang, M., Sun, H., Wang, X., Wang, Y., Li, Y., Zhang, L., Mu, Z., 2018b. Enhanced health risks from exposure to environmentally persistent free radicals and the oxidative stress of PM2.5 from asian dust storms in erenhot, Zhangbei and Jinan, China. Environ. Int. 123, 260−268.

Chen, Q., Wang, M., Wang, Y., Zhang, L., Li, Y., Han, Y., 2019e. Oxidative potential of water-soluble matter associated with chromophoric substances in PM2.5 over Xi'an, China. Environ. Sci. Technol, 53 (17), 10053−10061.

Chen, Q., Wang, M., Wang, Y., Zhang, L., Xue, J., Sun, H., Mu, Z., 2018c. Rapid determination of environmentally persistent free radicals (EPFRs) in atmospheric particles with a quartz sheet-based approach using electron paramagnetic resonance (EPR) spectroscopy. Atmos. Environ. 184, 140−145.

Cheng, Y., He, K. B., Du, Z. Y., Engling, G., Liu, J. M., Ma, Y. L., Zheng, M., Weber, R. J., 2016. The characteristics of brown carbon aerosol during winter in Beijing. Atmos. Environ. 127, 355–364.

534 Cormier, S. A., Lomnicki, S., Backes, W., Delligner, B., 2006. Origin and health impacts of
535 emissions of toxic by-products and fine particles from combustion and thermal treatment of
536 hazardous wastes and materials. Environ. Health. Perspect. 114 (6), 810−817.
537 D'Arienzo, M., Gamba, L., Morazzoni, F., Cosention, U., Creco, C., Lasagni, M., Pitea, D., Moro,
538 G., Cepek, C., Butera, V., Sicilia, E., Russo, N., Muñoz-García, A., Pavone, M., 2017.
539 Experimental and theoretical investigation on the catalytic generation of environmentally
540 persistent free radicals from benzene. J. Phys. Chem. A. 121 (17), 9381−9393.
541 Dellinger, B., Lomnicki, S., Khachatryan, L., Maskos, Z., Hall, R. W., Adounkpe, J., McFerrin, C.,
542 Truong, H., 2007. Formation and stabilization of persistent free radicals. Proc. Combust. Inst.
543 31 (1), 521−528.
544 Dellinger, B., Pryor, W. A., Cueto, R., Squadrito, G. L., Hegde, V., Deutsch, W. A., 2001. Role of
545 free radicals in the toxicity of airborne fine particulate matter. Chem. Res. Toxicol. 14 (10),
546 1371−1377.
547 Environmental Protection Agency, 1988. Recommendations for and Documentation of Biological
548 Values for Use in Risk Assessment. PB-179874. EPA 600/6-87/008. US Environmental
549 Protection Agency, Cincinnati, OH.
550 Finkelstein, E., Rosen, G. M., Rauckman, E. J., 1982. Production of hydroxyl radical by
551 decomposition of superoxide spin-trapped adducts. Mol. Pharmacol. 21 (2), 262–265.
552 Gehling, W., Dellinger, B., 2013. Environmentally persistent free radicals and their lifetimes in
553 PM2.5. Environ. Sci. Technol. 47 (15), 8172−8178.
554 Han, Y., Chen, Y. J., Saud, A., Feng, Y. L., Zhang, F., Song, W. H., Cao, F., Zhang, Y., Yang, X., Li,
555 J., Zhang, G., 2018. High time- and size-resolved measurements of PM and chemical
556 composition from coal combustion: Implications for the EC formation process. Environ. Sci.
557 Technol. 52 (11), 6676–6685.
558 Harmon, A. C., Hebert, V. Y., Cormier, S. A., Subramanian, B., Reed, J. R., Backes, W. L., Dugas,
559 T. R., 2018. Particulate matter containing environmentally persistent free radicals induces
560 AhRdependent cytokine and reactive oxygen species production in human bronchial
561 epithelial cells. Plos. One. 13 (10), e0205412.
562 Karnae, S., John, K., 2011. Source apportionment of fine particulate matter measured in an
563 industrialized coastal urban area of South Texas. Atmos. Environ. 45 (23), 3769−3776.
564 Keiluweit, M., Nico, P. S., Johnson, M. G., Kleber, M., 2010. Dynamic molecular structure of
565 plant biomass-derived black carbon (biochar). Environ. Sci. Technol. 44 (4), 1247−1253.
566 Khachatryan, L., Dellinger, B., 2011. Environmentally persistent free radicals (EPFRs)-2. Are free
567 hydroxyl radicals generated in aqueous solutions?. Environ. Sci. Technol. 45 (21),
568 9232−9239.
569 Li, G. L., Wu, S. Y., Kuang, M. Q., Hu, X. F., Xu, Y. Q., 2017. Studies on the g-factors of the
570 copper(II)-oxygen compounds. J. Struct. Chem. 58 (4), 700–705.
571 Lin, P., Hu, M., Deng, Z., Slanina, J., Han, S., Kondo, Y., Takegawa, N., Miyazaki, Y., Zhao, Y.,
572 Sugimoto, N., 2009. Seasonal and diurnal variations of organic carbon in PM2.5 in Beijing
573 and the estimation of secondary organic carbon. J. Geophys. Res-Atmos. 114, 1−41.
574 Liu, J., Bergin, M., Guo, H., King, L., Kotra, N., Edgerton, E., Weber, R. J., 2013. Size-resolved
575 measurements of brown carbon in water and methanol extracts and estimates of their
576 contribution to ambient fine-particle light absorption. Atmos. Chem. Phys. 13, 12389–12404.

Lomnicki, S., Truong, H., Vejerano, E., Dellinger, B., 2008. Copper oxide-based model of persistent free radical formation on combustion-derived particulate matter. Environ. Sci. Technol. 42 (13), 4982−4988.

Lyu, L., Yu, G., Zhang, L., Hu, C., Sun, Y., 2018. 4-Phenoxyphenolfunctionalized reduced graphene oxide nanosheets: A metal-free fenton-like catalyst for pollutant destruction. Environ. Sci. Technol. 52 (2), 747−756.

Lyons, M.J., Spence, J.B., 1960. Environmental free radicals. Br. J. Canc. 14, 703−708

Mihara, T., Michihiro, M., 2011. Characterization of solvent-extractable organics in urban aerosols based on mass spectrum analysis and hygroscopic growth measurement. Environ. Sci. Technol. 45 (21), 9168–9174.

Mukome, F. N. D., Zhang, X., Silva, L. C. R., Six, J., Parikh, S. J., 2013. Use of Chemical and physical characteristics to investigate trends in biochar feedstocks. J. Agric. Food Chem. 61 (9), 2196−2204.

Nikitenko, V. A., 1992. Luminescence and EPR of zinc oxide (review). J. Appl. Spectrosc. 57 (5–6), 783–798.

Oyana, T. J., Lomnicki, S. M., Guo, C., Cormier, S. A., 2017. A scalable field study protocol and rationale for passive ambient air sampling: a spatial phytosampling for leaf data collection. Environ. Sci. Technol. 51 (18), 10663−10673.

Pan, Y., Wang, Y., Sun, Y., Tian, S., Cheng, M., 2013. Size-resolved aerosol trace elements at a rural mountainous site in Northern China: importance of regional transport. Sci. total Environ. 461−462, 761−771.

Patterson, M. C., Keilbart, N. D., Kiruri, L. W., Thibodeaux, C. A., Lomnicki, S., Kurtz, R. L., Poliakoff, E. D., Dellinger, B., Sprunger, P. T., 2013. EPFR formation from phenol adsorption on Al2O3 and TiO2: EPR and EELS studies. Chem. Phys. 422, 277−282.

Pryor, W.A., Prier, D.G., Church, D.F., 1983. Electron-spin resonance study of mainstream and sidestream cigarette smoke: nature of the free radicals in gas-phase smoke and in cigarette tar. Environ. Health Perspect. 47, 345−355.

Pryor, W. A., 1986. Oxy-Radicals and Related Species: Their Formation, Lifetimes, and Reactions. Annu. Rev. Physiol. 48, 657–667.

Qi, L., Zhang, Y., Ma, Y., Chen, M., Ge, X., Ma, Y., Zheng, J., Wang, Z., Li, S., 2016. Source identification of trace elements in the atmosphere during the second Asian Youth Games in Nanjing, China: Influence of control measures on air quality. Atmos. Pollut. Res. 7, 547–556.

Shaltout, A. A., Boman, J., Shehadeh, Z. F., Al-Malawi, D. A. R., Hemeda, O. M., Morsy, M. M., 2015. Spectroscopic investigation of PM2.5, collected at industrial, residential and traffic sites in taif. Saudi Arabia. J. Aerosol. Sci. 79, 97−108.

Srivastava, A., Jain, V. K., 2007. Size distribution and source identification of total suspended particulate matter and associated heavy metals in the urban atmosphere of Delhi. Chemosphere. 68(3), 579−589.

Strak, M., Janssen, N. A. H., Godri, K. J., Gosens, I., Mudway, I. S., Cassee, F. R., Lebret, E., Kelly F. J., Harrison, R. M., Brunekreef, B., Steenhof, M., Hoek, G., 2012. Respiratory health effects of airborne particulate matter: The role of particle size, composition, and oxidative potential—the RAPTES project. Eviron. Health. Persp. 120 (8), 1183–1189.

Salma, I., Balásházy, I., Winkler-Heil, R., Hofmann, W., Záray, G. 2002. Effect of particle mass size distribution on the deposition of aerosols in the human respiratory tract. J. Aerosol. Sci. 33(1), 119-132.

Seabra A.B., Paula A.J., Lima R. D., Alves. O.L., Durán. N. 2014. Nanotoxicity of graphene and graphene oxide. Chem. Res. Toxicol. 27 (2), 159–168.

Thevenot, P. T., Saravia, J., Jin, N., Giaimo, J. D., Chustz, R. E., Mahne, S., Kelley, M. A., Hebert, V. Y., Dellinger, B., Dugas, T. R., Demayo, F. G., Cormier, S. A., 2013. Radical-containing ultrafine particulate matter initiates epithelial-to-mesenchymal transitions in airway epithelial cells. Am. J. Respir. Cell. Mol. Biol. 48 (2), 188−197.

Tian, H., Wang, Y., Xue, Z., Cheng, K., Qu, Y., Chai, F., Hao, J., 2010. Trend and characteristics of atmospheric emissions of Hg, As, and Se from coal combustion in China, 1980−2007. Atmos. Chem. Phys. 10 (23), 11905−11919.

Tong, H., Lakey, P. S. J., Arangio, A. M., Socorro, J., Shen, F., Lucas, K., Brune, W. H., Pöschl, U., Shiraiwa, M., 2018. Reactive oxygen species formed by secondary organic aerosols in water and surrogate lung fluid. Environ. Sci. Technol. 52 (20), 11642−11651.

Trapp, J. M., Millero, F. J., Prospero, J. M., 2010. Temporal variability of the elemental composition of African dust measured in trade wind aerosols at Barbados and Miami. Mar. Chem. 120 (1-4), 71−82.

Truong, H., Lomnicki, S., Dellinger, B., 2010. Potential for misidentification of environmentally persistent free radicals as molecular pollutants in particulate matter. Environ. Sci. Technol. 44 (6), 1933−1939.

Valavanidis, A., Fiotakis, K., Vlachogianni, T., 2008. Airborne particulate matterand human health: toxicological assessment and importance of size and composition of particles for oxidative damage and carcinogenic mechanisms. J. Environ. Sci. Heal. C. 26 (4), 339–362.

Vejerano, E. P., Rao, G., Khachatryan, L., Cormier, S. A., Lomnicki, S., 2018. Environmentally persistent free radicals: Insights on a new class of pollutants. Environ. Sci. Technol. 52 (5), 2468−2481.

Vejerano, E., Lomnicki, S. M., Dellinger, B., 2012a. Formation and stabilization of combustion-generated, environmentally persistent radicals on Ni(II)O supported on a silica surface. Environ. Sci. Technol. 46 (17), 9406−9411.

Vejerano, E., Lomnicki, S., Dellinger, B., 2011. Formation and stabilization of combustion-generated environmentally persistent free radicals on an Fe(III)2O3/silica surface. Environ. Sci. Technol. 45 (2), 589−594.

Valavanidis, A., Haralambous, E., 2001. A comparative study by electron paramagnetic resonance of free radical species in the mainstream and sidestream smoke of cigarettes with conventional acetate filters and 'bio-filters. Redox. Rep. 6, 161−171.

Vejerano, E., Lomnicki, S., Dellinger, B., 2010. Formation and stabilization of combustion-generated environmentally persistent free radicals on an Fe(III) 2O3/silica surface. Environ. Sci. Technol. 45 (2), 589−594.

Vejerano, E., Lomnicki, S., Dellinger, B., 2012b. Lifetime of combustion-generated environmentally persistent free radicals on Zn(II)O and other transition metal oxides. J. Environ. Monit. 14 (10), 2803−2806.

Wang, P., Pan, B., Li, H., Huang, Y., Dong, X., Fang, A., Liu, L., Wu, Min., Xing, B., 2018. The overlooked occurrence of environmentally persistent free radicals in an area with low-rank coal burning, Xuanwei, China. Environ. Sci. Technol. 52 (3), 1054−1061.

Wang, Y., Li, S., Wang, M., Sun, H., Mu, Z., Zhang, L., Li, Y., Chen, Q., 2019. Source apportionment of environmentally persistent free radicals (EPFRs) in PM2.5 over Xi'an, China. Sci. Total. Environ. 689, 193–202.

Yang, L., Liu, G., Zheng, M., Jin, R., Zhu, Q, Zhao, Y., Wu, X., Yang, X., 2017. Highly elevated levels and particle-size distributions of environmentally persistent free radicals in haze-associated atmosphere. Environ. Sci. Technol. 51 (14), 7936−7944.

Yu, T., Wang, J., Shen, M., Li, W., 2013. NH3-SCR over Cu/SAPO-34 catalysts with various acid contents and low Cu loading. Catal. Sci. Technol. 3 (12), 3234–3241.

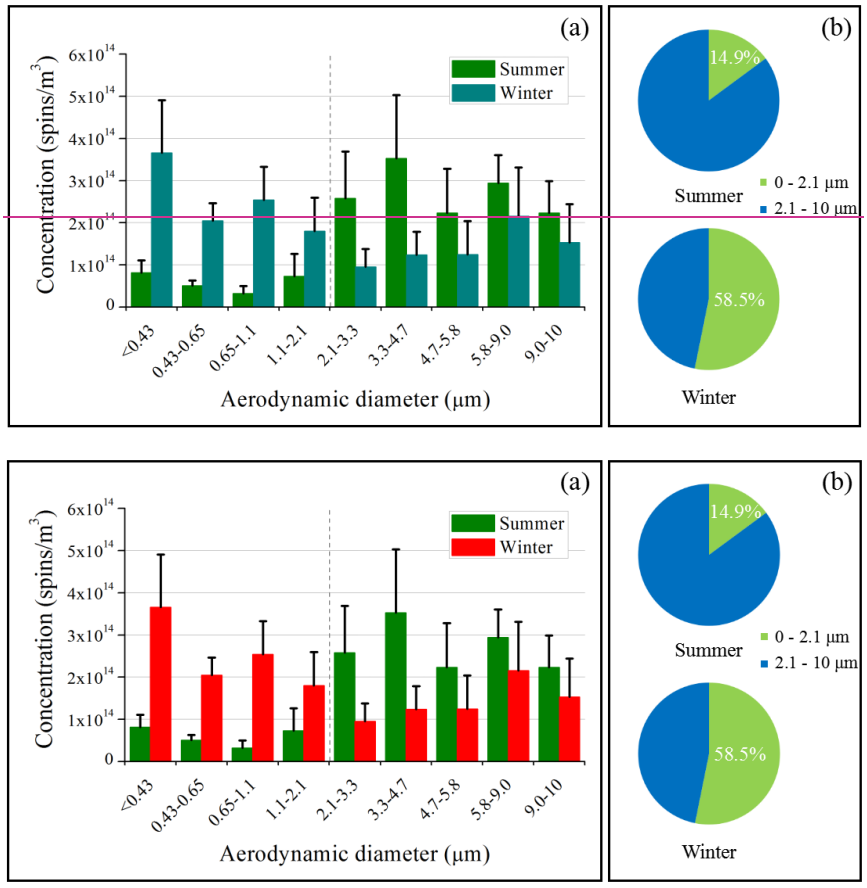

672

673

674 Figure 1. The concentration of EPFRs in PM with different particle sizes. (a) Atmospheric
675 concentrations of EPFRs in different particle sizes in summer and winter. (b) The relative
676 contribution of fine particles and coarse particles to the total EPFR concentration.

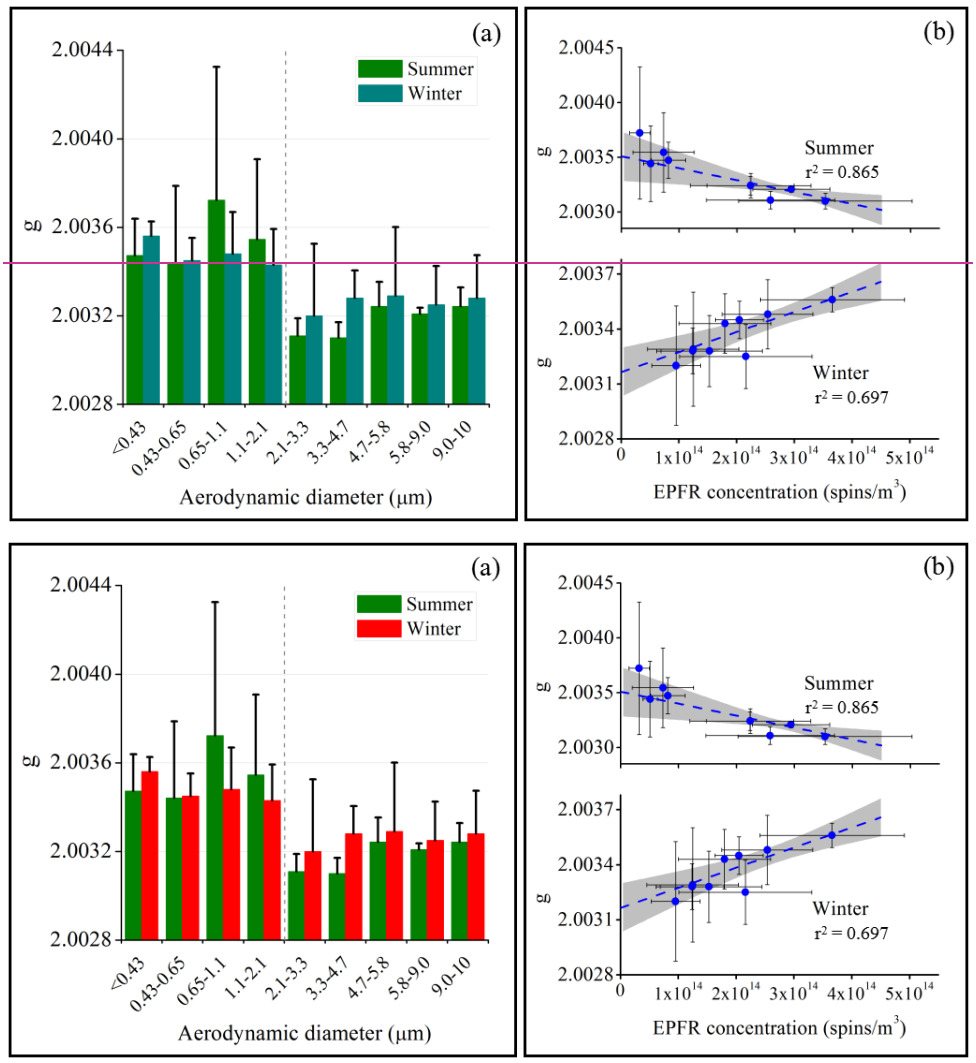

677

678

679 Figure 2. A *g*-factor comparison. (a) Comparison of *g*-factors of EPFRs in different particle sizes
680 in different seasons. (b) Correlation analysis of *g*-factors and concentrations of EPFRs in summer
681 and winter PM. The gray areas in the figure represent 95% confidence intervals.

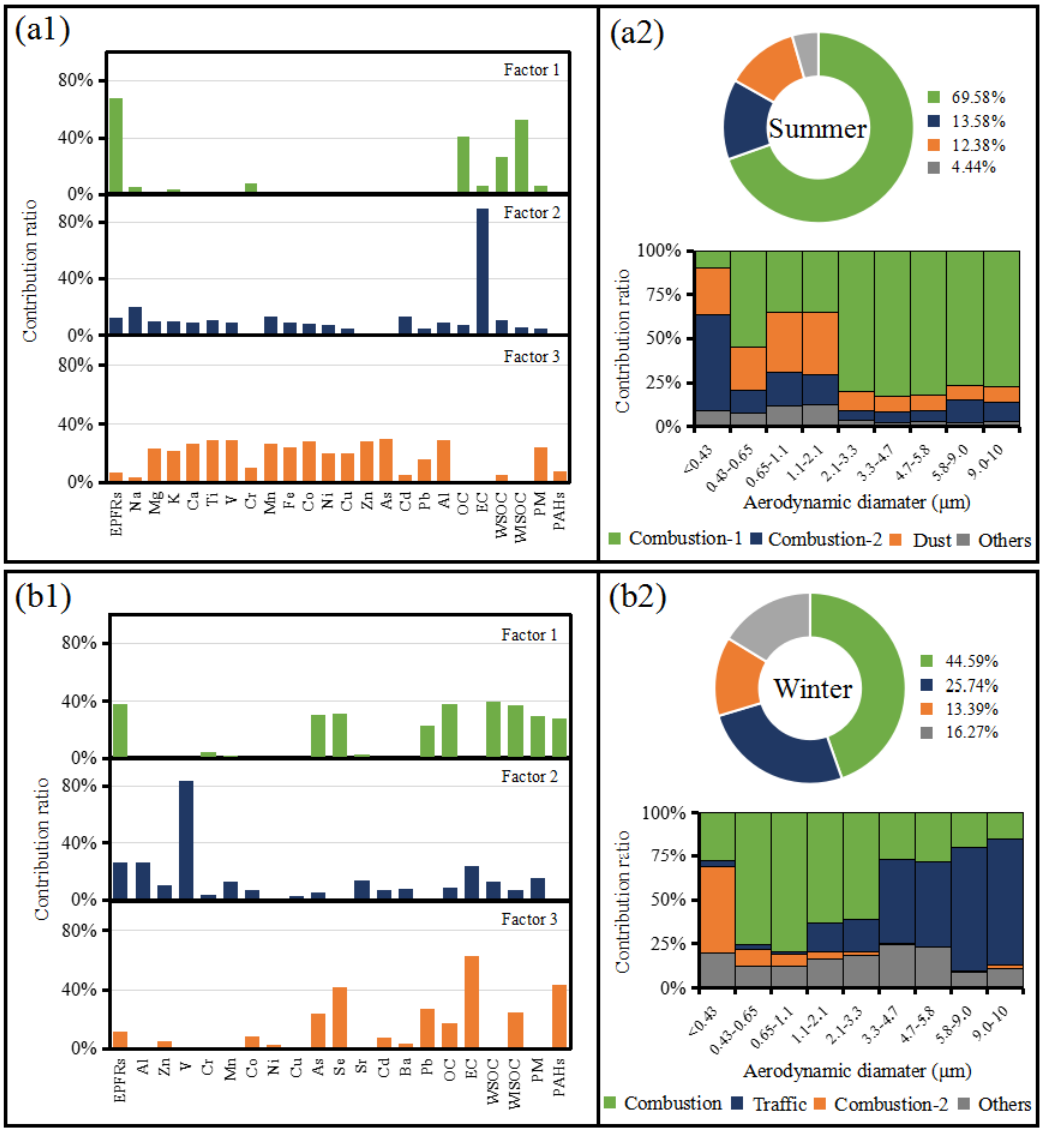

Figure 3. Factor analysis of EPFRs in different particle sizes in different seasons. (a1) and (b1) represent the results of factor analysis for summer and winter, respectively. (a2) and (b2) represent the contribution of various factors in summer and winter, respectively, to EPFRs and the relative contributions of each factor for different particle sizes.

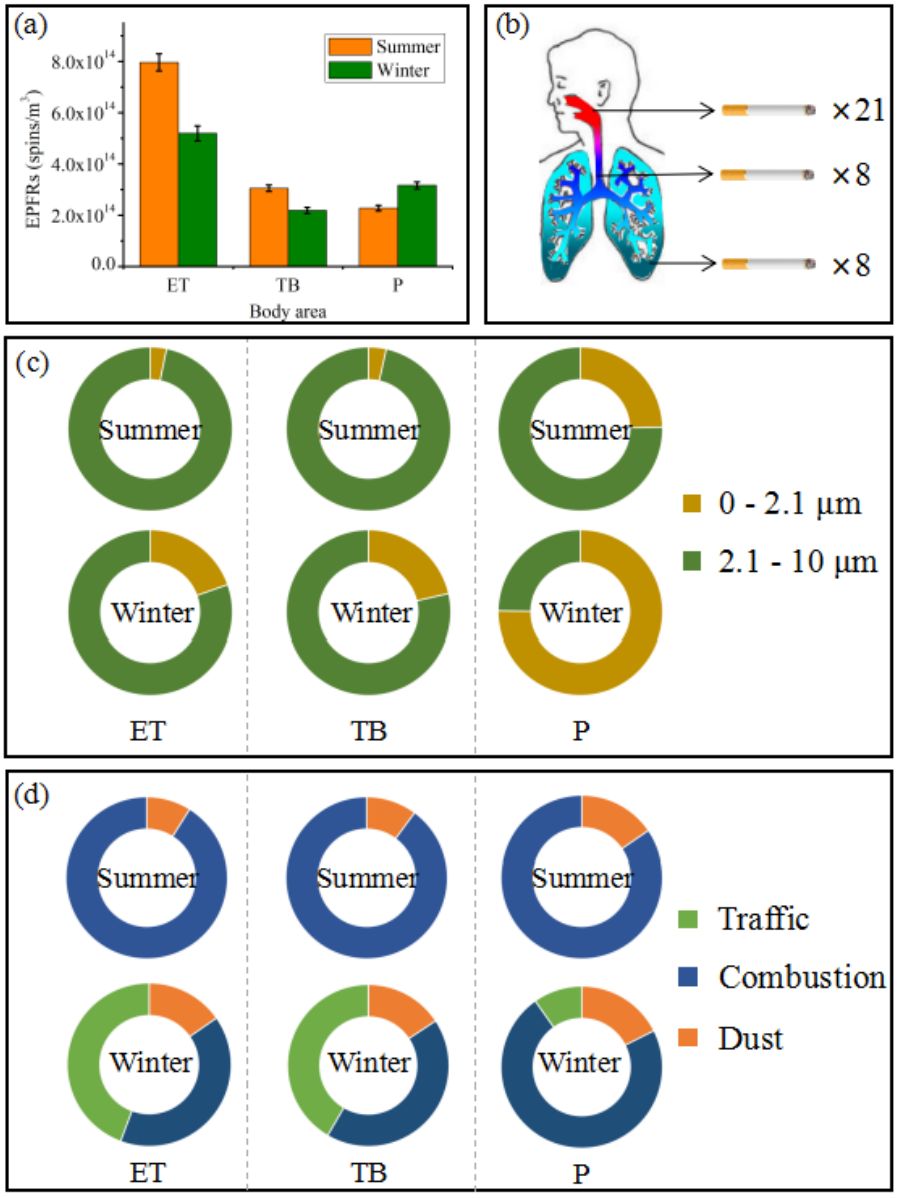

Figure 4. Exposure risks to EPFRs. (a) EPFR exposure in the ET, TB, and P regions. (b) Cigarette exposure to EPFRs in the human respiratory system. (c) Exposure ratio of EPFRs with different particle sizes in different areas of the respiratory system. (d) Contribution of EPFRs from different sources to different areas of the respiratory system.